Available online at www.sciencedirect.com

SciVerse ScienceDirect

journal homepage: www.elsevier.com/locate/jmbbm

Research paper

A numerical model for investigating the mechanics of calcaneal fat pad region

*A.N. Natali**, *C.G. Fontanella*, *E.L. Carniel*

University of Padova, Centre of Mechanics of Biological Materials, Via F. Marzolo 9, I-35131 Padova, Italy

ARTICLE INFO

Article history:
Received 28 March 2011
Received in revised form
19 May 2011
Accepted 30 August 2011
Published online 13 September 2011

Keywords:
Calcaneal fat pad
Soft tissue mechanics
Constitutive model
Numerical model

ABSTRACT

The present paper pertains to the definition of a numerical model of the calcaneal fat pad region, considering a structure composed of adipose and connective tissues organized in fibrous septae and adipose chambers. The mechanical response is strongly influenced by the structural conformation, as the dimension of adipose chambers, the thickness of connective septae walls and the mechanical properties of the different soft tissues. In order to define the constitutive formulation of adipose tissues, experimental data from pig specimens are considered, according to the functional similarity, while the mechanical response of connective tissue septae is assumed with regard to the mechanical behaviour that characterize ligaments. Different numerical models are provided accounting for the variation of chambers dimensions, septae wall thickness and tissues characteristics. The spiral angles of collagen fibres within the septae influence the capability of the structure to withstand the bulging of chambers. The analysis considers different orientation of the fibres. The response of calcaneal fat pad region is evaluated in comparison with experimental data from unconfined compression tests. The present work provides a preliminary approach to enhance the correlation between the structural conformation and tissues mechanical properties towards the biomechanical response of overall heel pad region.

1. Introduction

The calcaneal fat pad is a complex structure of adipose and connective tissues which surrounds the calcaneum in the posterior foot region. The mechanical role of the calcaneal fat pad tissues is to optimize the response to loading, for example by dumping shocks generated during gait or running cycle (Whittle, 1999) and makes it possible to achieve a smooth distribution of pressure field. In this way, the calcaneal fat pad configuration attempts the function of weight-bearing and shock-absorbing structure (Miller, 1982). The overall mechanical response of calcaneal fat pad region is influenced by the histologic and morphometric connective and adipose tissues configuration and by the structural conformation of the septal system (Buschmann et al., 1993; Natali et al., 2010). The mechanical response has been previously investigated by numerical formulations capable to interpret the overall behaviour of the structure. Phenomenological formulations were provided by different authors to specify the stress–strain relationship of tissues (Freed and Diethelm, 2006; Ledoux and Blevins, 2007; Miller-Young et al., 2002; Natali et al., 2010).

* *Corresponding author.* Tel.: +39 0 49 827 5598; fax: +39 0 49 827 5604.
E-mail addresses: arturo.natali@unipd.it, natali@dic.unipd.it (A.N. Natali).

1751-6161/$ - see front matter © 2011 Elsevier Ltd. All rights reserved.
doi:10.1016/j.jmbbm.2011.08.025

The calcaneal structure is complex and highly hierarchically organized, as dense strands of elastic fibrous tissue, which defines septae that binds adipose tissues in chambers of different sizes (Blechschmidt, 1982; Jahss et al., 1992a; Kuhns, 1949). Collagen fibres within septae are spirally arranged and superiorly fixed to bone or other septae, inferiorly to other septae of smaller size and to dermis. The adipose chambers contain packed fat cells which are arranged in lobules joined by connective tissues. Lobules are grouped by further bundles of collagen and elastin fibres (Jahss et al., 1992b). Adipose chambers' dimension and orientation depend on the specific location within the calcaneal region. Their dimension is small in the region close to dermis and progressively increases towards the calcaneal perichondrium (Hsu et al., 2007). In the central portion, the chambers are oriented vertically, while in the lateral and posterior regions are smaller and transversally oriented (Rome, 1998).

The stiffness of the calcaneal region is determined by the almost incompressible behaviour of adipose tissue bounded by collagen network (Torp-Pedersen et al., 2008). The spiral distribution of collagen fibres within connective septae is suitable to limit the bulging of chambers (Rome, 1998).

The calcaneal tissues' properties and the structural conformation provide an optimal mechanical response to the applied loads. Alterations caused by ageing or degenerative effects influence the mechanical properties of the tissue (Alcantara et al., 2002; Gefen et al., 2001; Hsu et al., 2009; Kwan et al., 2010; Pai and Ledoux, 2010; Tong et al., 2003; Tsai et al., 1999; Zheng et al., 2000). Degenerative phenomena can determine a gradual loss of collagen, a decrease in the quantity of elastic fibrous component and a reduction of liquid content. This is associated with a local loss of fat tissue and damage of fibrous tissue septae, through the distortion and the fragmentation of the fibrous proteins (Prichasuk et al., 1994). Furthermore, increased fat content correlated with obesity leads to increased pressure in the specific closed space and determines a growing local stiffness (Kuhns, 1949; Mirrashed et al., 2004). Pathologies, such as diabetic or atrophied phenomena, cause alterations in the ratio of saturated and unsaturated fatty acids, and determine a variation on the capability to withstand the stress. Fat globules decrease in size and number and also a reduction of the number of septal fibres takes place. Besides, the connective septae become thicker and contain a slightly higher percentage of fibrous tissues and assume a fragmented configuration (Buschmann et al., 1995; Gefen, 2010). In this condition, experimental tests confirm the presence of stiffer soft tissues, a less smooth plantar pressure distribution with higher local values and a reduction in the ability to absorb shock phenomena.

Based on the cylindrical specimens described by Miller-Young et al. (2002), a numerical model of the specimen, representative of calcaneal fat pad structure has been developed. The model accounts for the calcaneal fat pad configuration, as a structure composed of adipose and connective tissues organised in connective septae and adipose chambers. Different models are provided accounting for different chamber dimensions and setpae thickness, because of their influence on the overall mechanical response. Moreover the variation of the spiral angle of collagen fibres within the septae influences the capability of the structure to limit bulging of chambers and consequently different orientations of fibres are analysed. The aim of this work is to evaluate the response of fat pad region under unconfined compression tests, while considering the influence of structural conformation as chamber dimension, septal thickness and fibre orientation that can be related to histological changes induced by ageing and/or pathology.

The biomechanical contribution of adipose and connective tissues can be investigated on the basis of experimental data at disposal. Experimental tests performed on specimens from pig adipose tissues are considered because of the similarity with human ones (Comley and Fleck, 2010; Geerligs et al., 2008). The mechanical properties of connective tissue septae are considered to be similar to the mechanical behaviour of connective tissues, such as ligaments or tendons (Comley and Fleck, 2010). In this study, the constitutive formulation and the identification of constitutive parameters are evaluated adopting experimental tests performed on the anterior talofibular human ligament.

2. Methods

2.1. *Constitutive model for adipose tissue*

Experimental data from mechanical tests performed on adipose tissue show the strong non-linearity of the mechanical response, such as material and geometrical non-linearity, almost incompressible and time-dependent behaviour (Comley and Fleck, 2009, 2010; Geerligs et al., 2008). Different constitutive formulations are reported in literature for subcutaneous adipose tissues. With the aim of analysing the short time response, a hyperelastic constitutive model is adopted:

$$W(\mathbf{C}) = U(\mathbf{C}) + \tilde{W}(\mathbf{C})$$

where W is the hyperelastic potential. Considering the almost incompressible behaviour, the hyperelastic potential W can be split into volumetric U and iso-volumetric $\tilde{W}$ terms. The specific formulation developed is reported in more detail in Appendix A.

The evaluation of mechanical response of adipose tissues considers experimental tests on pig adipose tissue specimens that are used because of similarities in structural configuration and overall mechanical response with human tissues (Klein et al., 2007). Experimental data from compression tests on cylindrical specimens developed by Comley and Fleck (2009) are considered. In detail circular cylindrical specimen of adipose tissues are cut from jowl of the pigs (diameter 10 mm; height 3 mm) and compression tests are performed at different strain rates.

The identification of constitutive parameters, within the hyperelastic constitutive model developed, is obtained according to data from high strain rate tests. Due to the simple geometry of specimens and the uni-axial loading configuration, a preliminary analysis is performed by an analytical model that interprets the experimental conditions. The evaluation of constitutive parameters is performed by the minimization of a cost function which specifies

the discrepancy between experimental data and model results. The minimization takes into account a stochastic-deterministic procedure, such as described in Natali et al. (2009a).

2.2. Constitutive model for connective septae

The typical mechanical response of soft connective tissues, such as anisotropic behaviour, material and geometrical non-linearity, is determined by the complex configuration of the tissues themselves, as a composite material made of oriented fibres embedded within a ground matrix (Natali et al., 2009b). According to histological evidences, a fibre-reinforced hyperelastic model is adopted to interpret the mechanical behaviour of connective septae, accounting for different contributions from isotropic ground matrix and fibre families (Limbert and Taylor, 2002; Natali et al., 2008, 2009b; Ottani et al., 2001; Spencer, 1984; Weiss et al., 1996). The following general formulation of strain energy is adopted:

$$W(\mathbf{C}, \mathbf{a}_0^i \otimes \mathbf{a}_0^i) = W_m(\mathbf{C}) + \sum_{i=1}^{n} W_f^i(\mathbf{C}, \mathbf{a}_0^i \otimes \mathbf{a}_0^i)$$

where W_m is the term which specifies the isotropic ground matrix contribution, while W_f^i is the ith fibre family term and vector $\mathbf{a}_0^i$ is a unit vector that defines the fibre orientation. Notes concerning the specific constitutive formulation adopted are reported in Appendix B.

Mechanical tests are performed to determine the contribution of the ground matrix and the fibres on the overall mechanical response. In literature, different experimental tests are reported with regard to human tendons and ligaments that are considered (Funk et al., 2000; Wren et al., 2003) in order to determine the connective septae tissues properties. Tensile tests performed on ligaments of human foot are analysed (Attarain et al., 1985) assuming high strain rates in order to interpret the short time response of the tissue.

The fibre-reinforced hyperelastic model is considered and the constitutive parameters are evaluated, following the procedure described in Natali et al. (2009b).

2.3. Numerical model

A numerical model of a cylindrical specimen of calcaneal region has been developed in order to evaluate the influence of the septeal size and shape on the overall mechanical response during compression tests. The dimension of the region considered by the numerical model considers the specimen dimension reported by Miller-Young (2002), adopted in consideration of the accuracy and completeness. The numerical model is divided in adipose chambers tissue and connective septae tissue (as reported in Fig. 1). Assuming the dimensions reported in literature (Blechschmidt, 1982; Buschmann et al., 1993; Cichowitz et al., 2009; Robbins et al., 1989) and considering the measurements from MRI images, for healthy calcaneal fat pad tissue, the dimension of the adipose chambers ranges between 1.0 and 5.0 mm, while the thickness of the connective septae ranges between 0.8 and 2.0 mm. The configuration of calcaneal fat pad structure is assumed according to 2.4 mm adipose chambers

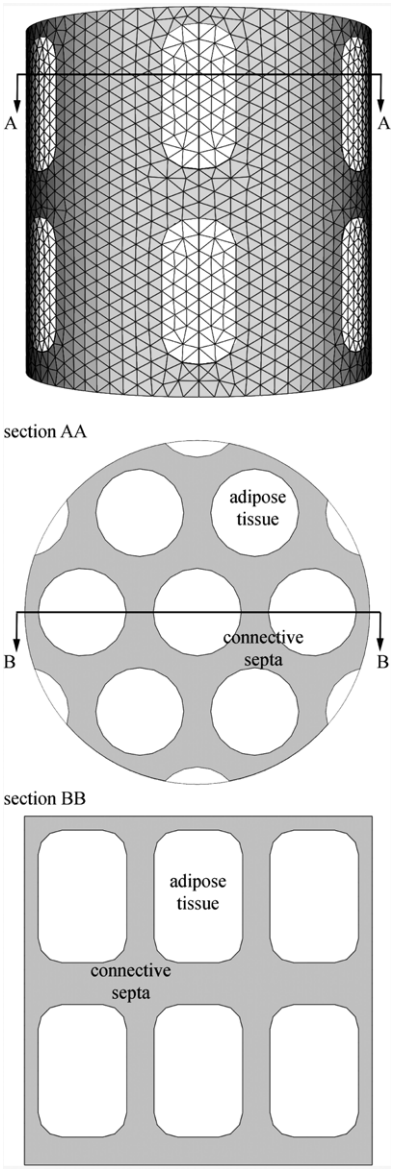

Fig. 1 – Numerical model of fat pad tissue (a), as adipose chambers and connective septae, according to the conformation shown in the transversal section (b) and the longitudinal section (c) reported.

diameter and about 1.0 mm connective septae thickness. The configuration of the adipose chambers is in agreement with the fact that the experimental specimens are taken in the central portion where the chambers are oriented vertically. The model is developed to report the unit reference volume that is representative of the specimen of the calcaneal region as performed in experimental tests.

The connective tissues septae are organized in fibres arranged spirally around the adipose chambers and numerical analyses are performed to evaluate the influence of the different orientations and distributions on mechanical response. In literature, a few details are reported about the orientation and direction of collagen fibres in the connective septae. However, the fibre orientation can be assumed according to other biological structures, which performs a similar mechanical func-

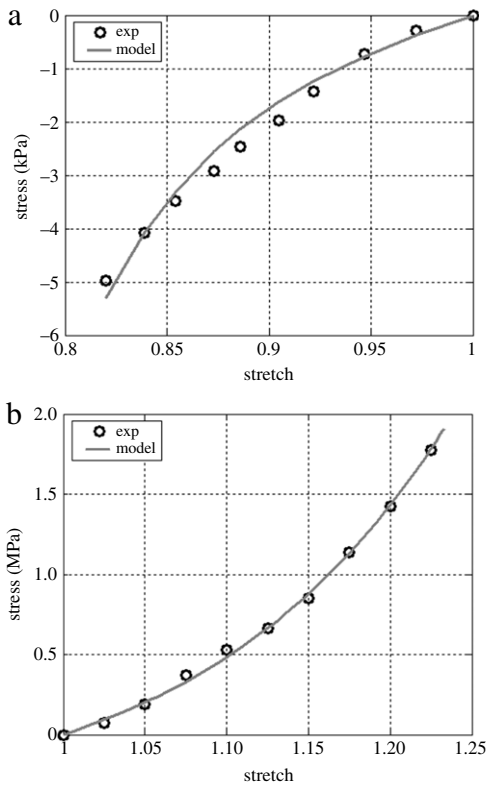

Fig. 2 – Comparison of experimental (empty dots) and model results (continuous lines): (a) compression tests on cylindrical pig adipose tissue specimens and (b) tensile tests on talo-fibular human ligament.

Table 1 – Hyperelastic parameters for adipose tissue (reference to Appendix A).

K_U (MPa)	r	C_1 (MPa)	α_1
2.31×10^{-1}	$2.74 \times 10^{+1}$	2.19×10^{-3}	5.35×10

Table 2 – Fibre-reinforced hyperelastic parameters for connective tissue (reference to Appendix B).

K_U (MPa)	C_1 (MPa)	C_4 (MPa)	α_4
2.02×10^{-2}	4.63×10^{-3}	2.36×10^{-1}	5.48×10

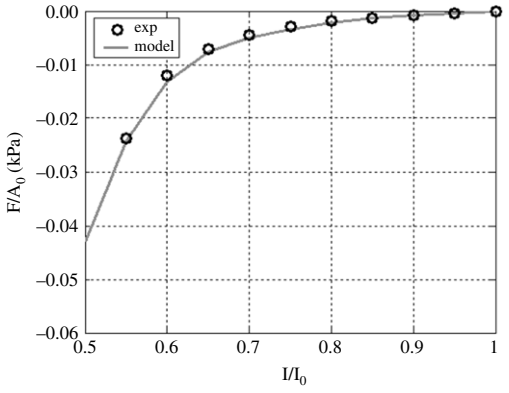

Fig. 3 – Comparison of experimental (empty dots) and model results (continuous lines) for unconfined compression tests on calcaneal fat pad samples at high strain rate (Miller-Young et al., 2002).

tion. For example, the fibre orientation of the human annulus fibrosus is in the range of 25°–45° to the transverse plane and located in different subsequent planes (Yin and Elliott, 2005). In this way, the most probable condition is described considering two groups of fibres distributed over the entire volume considered, one running in a clockwise and one in a anticlockwise direction. Different angles values are adopted as 15°, 30° and 45°, aiming also at a preliminary sensitivity evaluation of the response depending on this variation.

In order to evaluate the influence of structural conformations, different configurations of the numerical models have been developed starting from data obtained from literature and MRI investigation. Small chambers are assumed with the minor diameter of the chamber of 1.6 mm and the septae thickness of 1.8 mm, while larger chambers are assumed with the diameter of 3.0 mm and the septae thickness of 0.4 mm.

Numerical analyses are performed according to experimental conditions described by Miller-Young (2002). The numerical model is laterally unconstrained and squeezed between two steel platens. The bottom platen is fully fixed, while the top platen moves downward up to about 50% deformation. The friction coefficient at the contact interface of specimen and platens is 0.1 (Wu et al., 2004).

The hyperelastic constitutive models are implemented in the general purpose finite element software ABAQUS (Simulia, Dassault Systèmes, Providence, RI, USA) by developing ad hoc routines capable to interpret the behaviour of adipose and connective tissues, in consideration of the specific notes reported in Appendices A and B.

3. Results

The procedure adopted for the identification of the constitutive parameters follows the experience developed in the analysis of soft tissue mechanics (Natali et al., 2009a,b, 2010). In this context, the use of optimization procedure leads to the constitutive parameters reported in Tables 1 and 2, with regard to adipose tissues on pig specimen and anterior talofibular human ligament, respectively.

In Fig. 2, results are reported with regard to pig adipose tissue and on anterior talofibular human ligament specimens. Model results (continuous lines) are compared to experimental data from compression tests (Fig. 2(a)) showing the capability of the specific hyperelastic model to interpret the mechanical properties of adipose tissues. Model results (continuous lines) from tensile tests on connective tissues (Fig. 2(b)) are compared with experimental data on anterior talofibular ligament, also providing for a fitting of the constitutive parameters within the fibre-reinforced hyperelastic model adopted.

In Fig. 3, experimental data form Miller-Young et al. (2002) are compared with model results from numerical model of healthy configuration of calcaneal specimen. The correspondence of model results and the data reported by

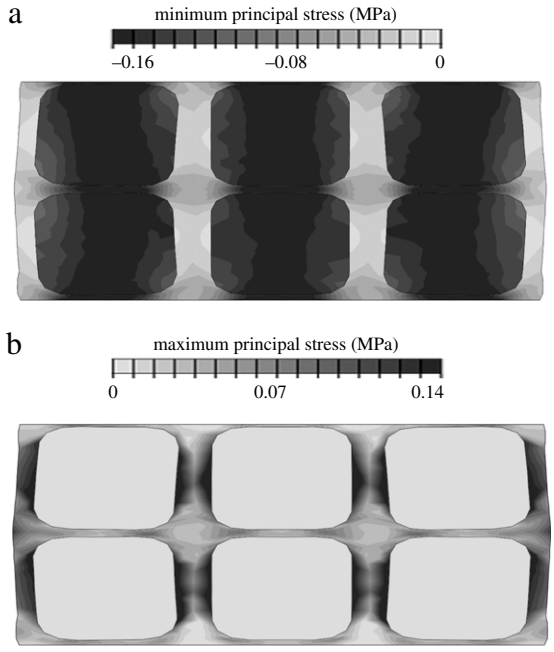

Fig. 4 – Results from the numerical model of calcaneal fat pad region: contours of minimum principal stress field (a) and maximum principal stress field for unconfined compression test, reported on a transversal section.

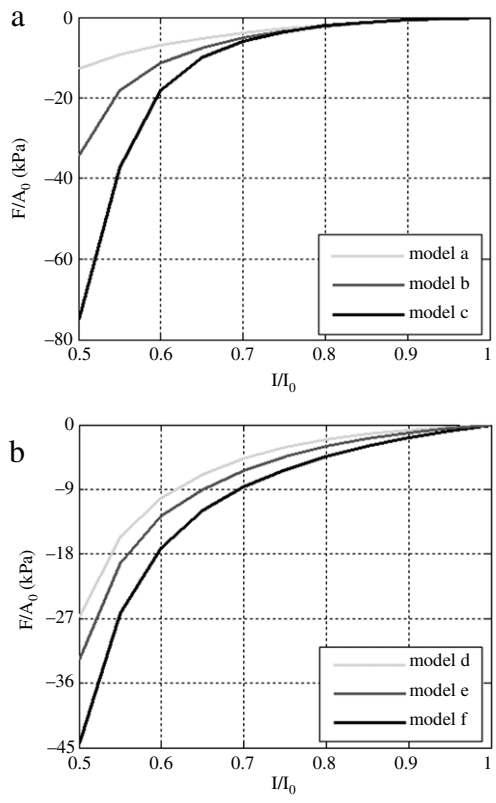

Fig. 5 – (a) The stress–strain relationship from the numerical analysis computed on models with different chamber dimension: small (model a), normal (model b) and large (model c) chambers. (b) The stress–strain relationship from the numerical analysis computed on models with different orientation of collagen fibres: 45° (model d), 30° (model e) and 15° (model f).

experimental data confirms the capability of the numerical model to interpret properly the problem investigated.

Deformed configurations of calcaneal region under unconfined compression tests (Fig. 4) are reported with regard to contours of minimum and maximum principal stress fields. In detail, Fig. 4(a) represents the minimum principal stress field that characterizes the response of the adipose chambers. Fig. 4(b) represents the contribute of connective septae in the overall response under compression.

Different numerical models of calcaneal region are developed to evaluate the influence of chambers dimension on mechanical behaviour. In Fig. 5(a), model results from different numerical models are reported. In detail, three different configurations of numerical models are reported: small chambers (model a), medium chambers (model b) and large chambers (model c). The increase of chamber dimensions, in association with septae configuration, provides a variation of the local stiffness. In Fig. 5(b), the stress–strain relationship is reported with regard to an angle of 45° (model d), 30° (model e) and 15° (model f) that the fibres form with the horizontal plane.

The mechanical behaviour of the tissues is underlined by the contour of maximum principal stress in Fig. 6. Particularly, the calcaneal fat pad specimen with big adipose chambers (Fig. 6(a)) provides higher values of stress on connective septae than normal adipose chambers (Fig. 6(b)).

In Fig. 7, contours of minimum and maximum principal stress fields in case of unconfined compression test for 15° (a)–(c) and 45° (b)–(d) collagen fibres orientation are reported, respectively.

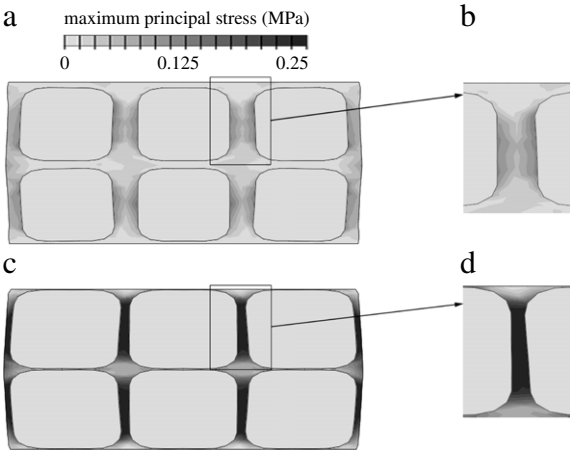

Fig. 6 – Results from the numerical analyses: contours of maximum principal stress field of unconfined compression test for normal (a)–(b) and large (c)–(d) chambers. Contours are reported on a transversal section of the fat pad numerical model.

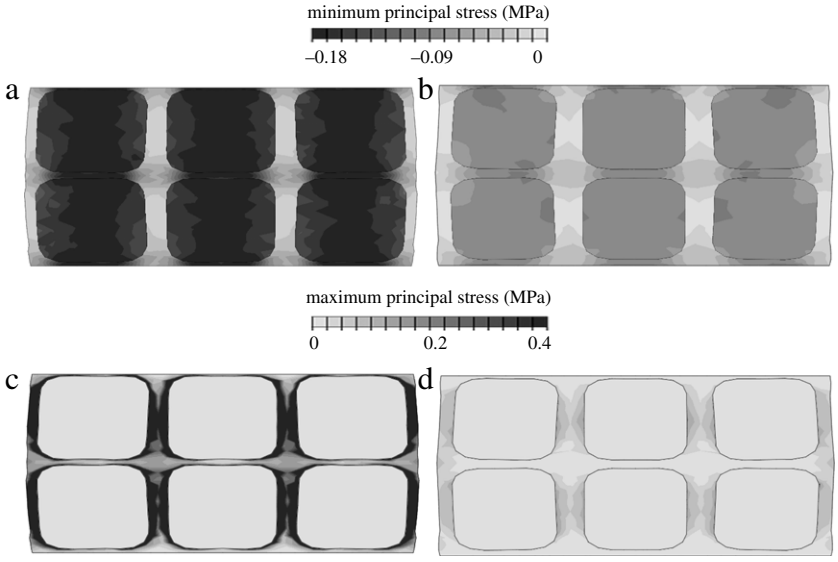

Fig. 7 – Results from the numerical analyses: contours of minimum principal stress field of unconfined compression test for 15° (a) and 45° (b) collagen fibres orientation and contours of maximum principal stress field of unconfined compression test for 15° (c) and 45° (d) collagen fibres orientation. Contours are reported on a transversal section of the fat pad numerical model.

4. Discussion

The peculiar structure of the calcaneal fat pad is able to provide a valid mechanical functionality under different loading conditions and in general to reduce potential injury to the body during gait cycle. The numerical model of calcaneal fat pad tissues developed proves to be able to interpret the correlation between the histologic and morphometric configuration, with regard to the adipose chambers and the connective septae, tissue mechanical properties and the overall mechanical response, by comparison with experimental data.

In particular, the results from numerical tests underline the mechanical contribution of adipose tissue and connective tissue on the mechanical response of the fat pad. The compressive stiffness of calcaneal fat pad structure is influenced by the adipose tissue, which is almost incompressible, together with the tension of fibrous septae that limit the bulging of the chambers themselves.

The influences of tissue mechanical properties as well as structural conformation are pointed out. The numerical models allow for the possibility to evaluate also the variation of the volume ratio between adipose chamber and fibrous septae and the mechanical properties of the tissues themselves.

The degenerative effects, due to age, trauma, or pathologies, such as diabetes or peripheral neuropathies, cause histologic changes in the heel pad structure of the foot. A change occurs in the chambers' dimension, septal thickness and fibres' orientation. These alterations determine variations in the mechanical behaviour of the heel pad region in terms of tissue biomechanical properties and structural conformation. Both terms must be evaluated to interpret the mechanical response.

Results from experimental investigations show the time dependence of fat pad tissues mechanical response that should be interpreted by viscoelastic models. The proposed formulation is defined accounting for data from mechanical tests performed at high strain rate, specifying the tissue instantaneous response. Hyperelastic formulations are adopted for this purpose.

This work represents a preliminary study which involves the correlation between tissue mechanics and structural conformation with regard to overall mechanical behaviour of calcaneal fat pad region and can represent, in spite of lack of reference data in literature, the basis for considering the influence of degeneration or pathological factors, as already in progress.

Acknowledgments

The authors received no financial support for the preparation of this manuscript and have no competing interests that are directly related to its contents.

Appendix A

The hyperelastic constitutive model is defined by the strain energy function $W(\mathbf{C})$ (Marsden and Hughes, 1968). The second Piola–Kircchoff stress tensor $\mathbf{S}$ is computed to satisfy thermodynamic requirement (Holzapfel, 2000; Simo and Hughes, 1998), as:

$$\mathbf{S}(\mathbf{C}) = 2\delta W(\mathbf{C})/\delta \mathbf{C}. \tag{A.1}$$

Almost-incompressible behaviour of the tissue is assumed and the strain energy function can be split into volumetric U and iso-volumetric $\tilde{W}$ contributions (Flory, 1961):

$$W(\tilde{I}_1, J) = U(J) + \tilde{W}(\tilde{I}_1) \tag{A.2}$$

where J is the deformation Jacobian, as $J = \sqrt{\det(\mathbf{C})}$, while $\tilde{I}_1$ is the first iso-volumetric invariant of the right Cauchy–Green strain tensor, as $\tilde{I}_1 = \mathrm{tr}(J^{-2/3}\mathbf{C})$. Because of the characteristic non-linearity of tissue response, specific polynomial and exponential functions are assumed to properly represent the trend of the energy components, as (Natali et al., 2004, 2008):

$$U(J) = \frac{K_v}{2 + r(r+1)}[(J-1)^2 + J^{-r} + rJ - (r+1)] \tag{A.3}$$

$$\tilde{W}(\tilde{I}_1) = \frac{C_1}{\alpha_1}\{\exp[\alpha_1(\tilde{I}_1 - 3)] - 1\}. \tag{A.4}$$

Constitutive parameters K_v and C_1 are related with the initial volumetric and shear stiffness, respectively. Parameters r and α characterize the evolution of material stiffness with strain because of the non-linearity of the mechanical response pointed out by mechanical tests.

Appendix B

With regard to the constitutive model adopted for connective septae, the hyperelastic formulation has to account for different contributions from fibres and isotropic ground matrix (Holzapfel, 2000; Limbert and Taylor, 2002; Spencer, 1984; Weiss et al., 1996):

$$W(J, \tilde{I}_1, I_4^i) = W_m(J, \tilde{I}_1) + \sum_{i=1}^{n} W_f^i(I_4^i) \tag{B.1}$$

where W_m is the term which specifies the isotropic ground matrix, while W_f^i specifies the mechanical response of the ith fibre family. I_4^i is a structural invariant related to the direction $\mathbf{a}_0^i$ assumed by fibres because of stretch, as $I_4^i = \mathbf{a}_0^i \cdot \mathbf{C}\mathbf{a}_0^i = (\lambda^i)^2$. Because of the predominant role of the fibres, a neo-Hookean formulation can be assumed to interpret the mechanical response of ground matrix, as almost-incompressible materials:

$$W_m(J, \tilde{I}_1) = K_v(J-1)^2 + C_1(\tilde{I}_1 - 3)^2 \tag{B.2}$$

where K_v can be related to the volumetric stiffness, while C_1 is associated to the tissue shear stiffness. The mechanical contribution of fibres can be described considering their structural organization (Ottani et al., 2001). In the unstrained configuration, fibres are characterised by a wavy conformation. When tensile load is applied, fibres first uncrimp and then get stretched. This mechanism determines a strongly non-linear mechanical response that can be described by an exponential formulation (Natali et al., 2004):

$$W_f^i(I_4^i) = \frac{C_4}{\alpha_4^2}\{\exp[\alpha_4(I_4^i - 1)] - \alpha_4(I_4^i - 1) - 1\} \tag{B.3}$$

where C_4 is a constant that defines the fibres initial stiffness, as $E_f = 4C_4$, while α_4 depends on the initial wavy conformation of fibres (Natali et al., 2008). The number of fibre families is evaluated according to tissue histology.

REFERENCES

Alcantara, E., Foner, A., Ferrùs, E., Garcià, A.C., Ramiro, J., 2002. Influence of age, gender and obesity on the mechanical properties of the heel pad under walking impact conditions. J. Appl. Biomed. 18, 345–356.

Attarain, D.E., McCrackin, H.J., DeVito, D.P., McElhaney, J.H., Garret, W.E., 1985. Foot Ankle 6 (2), 54–58.

Blechschmidt, E., 1982. The structure of the calcaneal padding. Foot Ankle 2 (5), 260–283.

Buschmann, W.R., Hudgins, L.C., Kummer, F., Desai, P., Jahss, M.H., 1993. Fatty acid composition of normal and atrophied heel fat pad. Foot Ankle 14 (7), 389–394.

Buschmann, W.R., Jahss, M.H., Kummer, F., Desai, P., Gee, R.O., Ricci, J.L., 1995. Histology and histomorphometric analysis of the normal and atrophic heel fat pad. Foot Ankle Int. 16 (5), 254–258.

Cichowitz, A., Pan, W.R., Ashton, M., 2009. The heel. Anatomy, blood supply, and the pathophysiology of pressure ulcers. Ann. Plast. Surg. 62 (4), 423–429.

Comley, K., Fleck, N.A., The high strain rate response of adipose tissue. Iutam Symposium on Mechanical Properties of Cellular Materials. vol. 12. 2009. pp. 27–33.

Comley, K., Fleck, N.A., 2010. A micromechanical model for the Young's modulus of adipose tissue. Internat. J. Solids Structures 47, 2982–2990.

Flory, P.J., 1961. Thermodynamic relations for high elastic materials. Trans. Faraday Soc. 57, 829–838.

Freed, A.D., Diethelm, K., 2006. Fractional calculus in biomechanics: a 3D viscoelastic model using regularized fractional derivative kernels with application to the human calcaneal fat pad. Biomech. Model. Mechanobiol. 5 (4), 203–215.

Funk, J.R., Hall, G.W., Crandall, J.R., Pilkey, W.D., 2000. Linear and quasi-linear visco-elastic characterization of ankle ligament. J. Biomed. Eng. 122, 15–22.

Geerligs, M., Peters, G.W.M., Ackermans, P.A.J., Oomens, C.W.J., Baaijens, F.P.T., 2008. Linear viscoelastic response of adipose tissue. Biorheology 45 (6), 677–688.

Gefen, A., 2010. The biomechanics of heel ulcers. J. Tissue Viability 19 (4), 124–131.

Gefen, A., Megido-Ravid, M., Azariah, M., Itzchak, Y., Arcan, M., 2001. Integration of plantar soft tissue stiffness measurements in routine MRI of diabetic foot. Clin. Biomech. 16, 921–1025.

Holzapfel, G.A., 2000. Non Linear Solid Mechanics—A Continuum Approach for Engineering. John Wiley & Sons Ltd., New York

Hsu, C.C., Tsai, W.C., Hsiao, T.Y., Tseng, F.Y., Shau, Y.W., Wang, C.L., Lin, S.C., 2009. Diabetic effects on microchambers and macrochambers tissue properties in human heel pad. Clin. Biomech. 24, 682–686.

Hsu, C.-C., Tsai, W.-C., Wang, C.-L., Pao, S.-H., Shau, Y.-W., Chuan, Y.-S., 2007. Microchambers and macrochambers in heel pads: are they functionally different? J. Appl. Physiol. 102, 2227–2231.

Jahss, M.H., Michelson, J.D., Desai, P., Kaye, R., Kummer, F., Buschman, W., Watkins, F., Reich, S., 1992b. Investigations into the fat pads of the sole of the foot: anatomy and histology. Foot Ankle Int. 13, 227–232.

Jahss, M.H., Michelson, J.D., Kummer, F., 1992a. Investigations into the fat pads of the sole of the foot: heel pressure studies. Foot Ankle Int. 13, 233–242.

Klein, J., Permana, P.A., Owecki, M., Chaldakov, G.N., Bohm, M., Hausman, G., Lapiere, C.M., Atanassova, P., Sowinski, J., Fasshauer, M., Hausman, D.B., Maquoi, E., Tonchev, A.B., Peneva, V.N., Vlachanov, K.P., Fiore, M., Aloe, L., Slominski, A., Reardon, C.L., Ryan, T.J., Pond, C.M., 2007. What are subcutaneous adipocytes really good for y?. Experimental Dermatology 16, 45–70.

Kuhns, J.G., 1949. Changes in elastic adipose tissue. J. Bone Joint Surg. Am. 31, 541–547.

Kwan, R.LC., Zheng, Y.P., Cheing, G.LY., 2010. The effect of aging on the biomechanical properties of plantar soft tissues. Clin. Biomech. 25 (6), 601–605.

Ledoux, W.R., Blevins, J.J., 2007. The compressive material properties of the plantar soft tissue. J. Biomech. 40, 2975–2981.

Limbert, G., Taylor, M., 2002. On the constitutive modeling of biological soft connective tissues: a general theoretical framework and explicit forms of the tensors of elasticity for strongly anisotropic continuum fiber-reinforced composites at finite strain. Internat. J. Solids Structures 39, 2343–2358.

Marsden, J.E., Hughes, T.J.R., 1968. Mathematical Foundations of Elasticity. Prentice Hall, Englewood Cliffs, New Jersey.

Miller, W.E., 1982. The heel pad. Am. J. Sports Med. 10 (1), 19–21.

Miller-Young, J.E., Duncan, N.A., Baroud, G., 2002. Material properties of the human calcaneal fat pad in compression: experiment and theory. J. Biomech. 35, 1523–1531.

Mirrashed, F., Sharp, J.C., Krause, V., Morgan, J., Tomanek, B., 2004. Pilot study of dermal and subcutaneous fat structures by MRI in individuals who differ in gender, BMI, and cellulite grading. Skin Res. Technol. 10, 161–168.

Natali, A.N., Carniel, E.L., Gregersen, H., 2009b. Biomechanical behaviour of oesophageal tissues: material and structural configuration, experimental data and constitutive analysis. Med. Eng. Phys. 31, 1056–1062.

Natali, A.N., Carniel, E.L., Pavan, P.G., Sander, F.G., Dorow, C., Geiger, M., 2008. A visco-hyperelastic-damage constitutive model for the analysis of the biomechanical response of the periodontal ligament. ASME J. Biomech. Eng. 130 (3), 031004.

Natali, A.N., Fontanella, C.G., Carniel, E.L., 2010. Constitutive formulation and analysis of heel pad tissues mechanics. Med. Eng. Phys. 32, 516–522.

Natali, A.N., Forestiero, A., Carniel, E.L., 2009a. Parameters identification in constitutive models for soft tissue mechanics. Russian J. Biomech. 13 (4), 29–39.

Natali, A.N., Pavan, P.G., Carniel, E.L., Dorow, C., 2004. Viscoelastic response of the periodontal ligament: an experimental-numerical approach. J. Connect. Tissue. Res. 45, 222–230.

Ottani, V., Raspanti, M., Rugeri, A., 2001. Collagen structure and functional implications. Micron 32, 251–260.

Pai, S., Ledoux, W.R., 2010. The compressive mechanical properties of diabetic and non-diabetic plantar soft tissue. J. Biomech. 43 (9), 1754–1760.

Prichasuk, S., Mulpruek, P., Siriwongpairat, P., 1994. The heel pad compressibility. Clin. Orthop. Relat. R. 300, 197–200.

Robbins, S.E., Gouw, G.J., Hanna, A.M., 1989. Running-related injury prevention through innate impact-moderating behavior. Med. Sci. Sports Exerc. 21 (2), 130–139.

Rome, K., 1998. Mechanical properties of the heel pad: current theory and review of the literature. Foot 8, 179–185.

Simo, J.C., Hughes, T.J.R., 1998. Computational Inelasticity. Springer, New York.

Spencer, A.J.M., 1984. Continuum Theory of the Mechanics of Fibre-Reinforced Composites. Springer-Verlag, New York.

Tong, J., Lim, C.S., Goh, O.L., 2003. Technique to study the biomechanical properties of the human calcaneal heel pad. Foot 13, 83–91.

Torp-Pedersen, S.T., Matteoli, S., Wilhjelm, J.E., Amris, K., Bech, J.I., Christensen, R., Danneskiold-Samsøe, B., 2008. Diagnostic accuracy of heel pad palpation—a phantom study. J. Forensic Leg. Med. 15, 437–442.

Tsai, W.C., Wang, C.L., Hsu, T.C., Hsieh, F.J., Tang, F.T., 1999. The mechanical properties of the heel pad in unilateral plantar heel pain syndrome. Foot Ankle Int. 20 (10), 663–668.

Weiss, J.A., Maker, B.N., Govindjee, S., 1996. Finite element implementation of incompressible, transversely isotropic hyperelasticity. Comput. Method. Appl. M. 135, 107–128.

Whittle, M.W., 1999. Generation and attenuation of transient impulsive forces beneath the foot: a review. Gait Posture 10, 264–275.

Wren, T.A.L., Lindsey, D.P., Beauprè, G.S., Carter, D.R., 2003. Effects of creep and cyclic loading on the mechanical properties and failure of human Achilles tendons. Ann. Biomed. Eng. 331, 710–717.

Wu, J.W., Dong, R.G., Schopper, A.W., 2004. Analysis of effects of friction on the deformation behaviour of soft tissues in unconfined compression tests. J. Biomech. 37, 147–155.

Yin, L., Elliott, D.M., 2005. A homogenization model of the annulus fibrosus. J. Biomech. 38, 1674–1684.

Zheng, Y.P., Choi, Y.K.C., Wong, K., Chan, S., Mak, A.F.T., 2000. Biomechanical assessment of plantar foot tissue in diabetic patients using an ultrasound indentation system. Ultrasound Med. Biol. 26, 451–456.